Rapid Communication

Mitochondrial Dysfunction Contributes to Alveolar Developmental Arrest in Hyperoxia-Exposed Mice

Veniamin Ratner[1], Anatoly Starkov[2], Dzmitry Matsiukevich[1], Richard A. Polin[1], and Vadim S. Ten[1]

[1]Department of Pediatrics, Columbia University, New York, New York; and [2]Department of Neurology, Weill Medical College, Cornell University, New York, New York

This study investigated whether mitochondrial dysfunction contributes to alveolar developmental arrest in a mouse model of bronchopulmonary dysplasia (BPD). To induce BPD, 3-day-old mice were exposed to 75% O_2. Mice were studied at two time points of hyperoxia (72 h or 2 wk) and after 3 weeks of recovery in room air (RA). A separate cohort of mice was exposed to pyridaben, a complex-I (C-I) inhibitor, for 72 hours or 2 weeks. Alveolarization was quantified by radial alveolar count and mean linear intercept methods. Pulmonary mitochondrial function was defined by respiration rates, ATP-production rate, and C-I activity. At 72 hours, hyperoxic mice demonstrated significant inhibition of C-I activity, reduced respiration and ATP production rates, and significantly decreased radial alveolar count compared with controls. Exposure to pyridaben for 72 hours, as expected, caused significant inhibition of C-I and ADP-phosphorylating respiration. Similar to hyperoxic littermates, these pyridaben-exposed mice exhibited significantly delayed alveolarization compared with controls. At 2 weeks of exposure to hyperoxia or pyridaben, mitochondrial respiration was inhibited and associated with alveolar developmental arrest. However, after 3 weeks of recovery from hyperoxia or 2 weeks after 72 hours of exposure to pyridaben alveolarization significantly improved. In addition, there was marked normalization of C-I and mitochondrial respiration. The degree of hyperoxia-induced pulmonary simplification and recovery strongly ($r^2 = 0.76$) correlated with C-I activity in lung mitochondria. Thus, the arrest of alveolar development induced by either hyperoxia or direct inhibition of mitochondrial oxidative phosphorylation indicates that bioenergetic failure to maintain normal alveolar development is one of the fundamental mechanisms responsible for BPD.

Keywords: bronchopulmonary dysplasia; hyperoxia; mitochondrial dysfunction; bioenergetic failure

Bronchopulmonary dysplasia (BPD) is one of the most devastating complications of prematurity. Clinical studies have identified numerous risk factors for development of BPD in premature infants, including hyperoxia, ventilator-induced pulmonary injury, and prenatal and antenatal infection (1, 2). Despite attempts to avoid excessive oxygen supplementation, restrict fluids, prevent infection, and use "gentle" ventilation techniques, the incidence of BPD has not changed significantly. Although the development of BPD has been associated with a wide variety of risk factors, the histopathologic end-point of this disease is the same—an arrest of alveolar development. This implies the existence of a fundamental mechanism responsible for arrest of alveolarization when actively developing lungs are subjected to stress.

Compared with other age groups, premature neonates exhibit the highest total energy expenditure secondary to an accelerated growth rate. Growth restriction, delayed bone mass accretion (3, 4) and delayed catch-up growth (5, 6) are well documented in infants who develop chronic lung disease. Clinical trials have failed to demonstrate that an early increase in caloric intake can attenuate the incidence of BPD in very low birth weight premature infants (7, 8).

Mitochondria are the only organelles to provide cells with energy. It has been reported that mitochondrial function is essential for normal growth in pulmonary epithelial-like cells in culture (9). Compromised mitochondrial oxidative phosphorylation has been implicated in pathogenesis of genetic diseases presenting with developmental and growth restriction of different organs (10). Clearly, well-functioning mitochondria are needed to convert nutritional substrates into energy to maintain growth and development. We hypothesized that alveolar developmental arrest in premature neonates with BPD is secondary to mitochondrial bioenergetic failure to maintain normal pulmonary development.

MATERIALS AND METHODS

The Model of BPD and Study Groups

The model of BPD was produced in 3-day-old (Postnatal Day [P]3) neonatal mice as described (11) with minor modification. P3 mice (C57Bl/6J) with their dams were purchased from Jackson Laboratories (Bar Harbor, ME). At this age, mouse lungs are at the saccular stage of development that corresponds to lung development at 28 to 32 weeks of gestation in the human fetus (12). All pups from different litters were randomly distributed (six pups per dam). To produce lung injury, mice were exposed to 75% O_2. The experimental protocol was approved by Columbia University Institutional Animal Care and Use Committee. Mice were killed at three different time points (Figure 1A): at 72 hours of hyperoxia (Group #1), at the end of the 2 weeks of hyperoxia (Group #2), and at 3 weeks of recovery in RA after 2 weeks of hyperoxic exposure (Group #3). In each group of mice, lungs were examined for the degree of alveolarization. In the same mice, pulmonary mitochondria were isolated and assessed for respiratory function and activity of C-I. Data were compared with naïve littermates and between groups.

To determine if direct inhibition of mitochondrial respiratory chain results in alveolar simplification, an additional cohort of mice was exposed to pyridaben, a selective inhibitor of C-I activity (13). Pyridaben in dimethyl sulfoxide (DMSO and normal saline 1:1) was injected subcutaneusly at the dose 4 mg/kg daily. Control littermates received vehicle (the same volume of DMSO/normal saline). At 72 hours of exposure, randomly selected mice were killed and their pulmonary mitochondrial function (respiration rates and ATP production rates) and alveolar development were compared with that in vehicle-treated littermates. At 72 hours of pyridaben exposure, mice were divided into two groups. In Group 1, mice continued to receive pyridaben; in Group 2,

(*Received in original form September 2, 2008 and in final form December 11, 2008*)

Correspondence and requests for reprints should be addressed to Vadim S. Ten, M.D., Ph.D., Department of Pediatrics, Columbia University, 3959 Broadway, CHN 1201, New York, NY 10032. E-mail: vt82@columbia.edu

Am J Respir Cell Mol Biol Vol 40. pp 511–518, 2009
Originally Published in Press as DOI: 10.1165/rcmb.2008-0341RC on January 23, 2009
Internet address: www.atsjournals.org

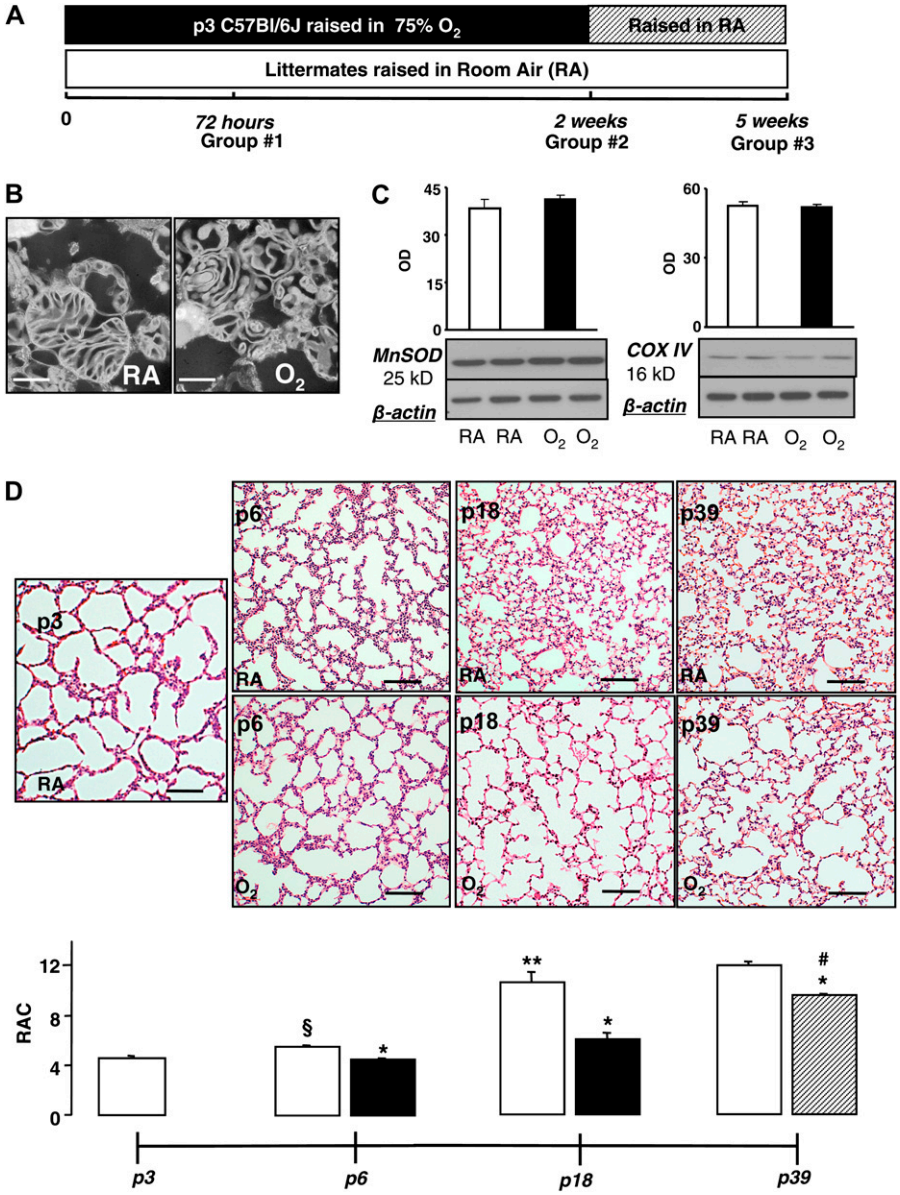

Figure 1. (*A*) Experimental timeline and design. (*B*) Electron microscopy of pulmonary mitochondria isolated from naïve and hyperoxic Postnatal Day (P)18 mice. *Scale bar* = 500 nm. (*C*) Immunoblots of representative samples from naïve (room air [RA]-exposed) and O_2-exposed mice and optical density graphs of MnSOD and COX IV expression in mitochondrial isolates from naïve P18 mice (*open bars*, $n = 4$) and P18 mice subjected to hyperoxia for 2 weeks (*solid bars*, $n = 4$). (*D* and *E*) Representative images of hematoxylin and eosin–stained lung sections with corresponding radial alveolar count (RAC) analysis; in naïve mice (*open bars*, P3 $n = 4$, P6 $n = 7$, P18 $n = 10$, P39 $n = 4$), mice subjected to hyperoxia (*solid bars*, P6 $n = 8$, P18 $n = 8$), and recovery (*hatched bar*, P39 $n = 4$). *Scale bar* = 500 μm. Data are mean ± SEM. $^{*}P \leq 0.002$ compared with naïve littermates, $^{**}P = 0.0001$ compared with naïve P6 mice, $^{\#}P < 0.0001$ compared with P6 and P18 hyperoxia-exposed mice, $^{\S}P = 0.0003$ compared with P3 naïve mice.

the pyridaben exposure was discontinued and mice were raised in room air. At 2 weeks of age lungs were harvested for assessment of alveolar development and mitochondrial function.

Assessment of Pulmonary Alveolarization

After a thoracotomy, the left atrium was transected and the main pulmonary artery was perfused transcardially with 1 ml of mitochondrial isolation buffer (*see below*).

The trachea was filled with the same buffer under a pressure of 20 cm H_2O for 1 minute. The left hilus was clipped and the right lung was excised for isolation of mitochondria. The left lung was fixed in 4% paraformaldehyde and embedded in paraffin. Three 5-μm sections were obtained from anterior, middle, and posterior frontal planes 100 μm apart from each other and stained with hematoxylin and eosin (H&E). An investigator blind to the study design performed morphometric assessment of digital images captured under identical magnification (×10). Two different methods were used to assess alveolarization. (*1*) Radial alveolar count (RAC) was the number of distal air sacs that were transected by the line drawn from the most distal terminal bronchiole toward the nearest pleura (14, 15). (*2*) Mean linear intercept (Lm) was measured by dividing the length of a line drawn across the lung section by the total number of septal wall intercepts encountered in 30 lines (40 μm apart) per lung image (16). Three measurements were obtained from each section (nine RACs/Lms per single mouse). The mean values were used for statistical analysis.

Isolation of Pulmonary Mitochondria

To isolate mitochondria from a single lung, we modified a method for isolation of brain mitochondria in neonatal mice (17). Briefly, lung tissue was homogenized in 3 ml of isolation buffer (IB) using a dounce homogenizer (Wheaton Ind., Millville, NJ) with 0.2 mm differential (20 strokes), followed by 0.1 mm differential (10 strokes) and transferred into three 1.5-ml tubes. The homogenate was centrifuged at 1,100 × *g* for 2 minutes at 4°C. The 0.750 ml of supernatant was mixed with 0.07 ml of 80 vol% Percoll, carefully layered on top of 0.7 ml of 10% Percoll, and centrifuged at 18,500 × *g* for 10 minutes. The mitochondria-enriched fraction was collected at the bottom of the tube, resuspended in 1.0 ml of washing buffer, and centrifuged at 10,000 × *g* for 5 minutes. The final mitochondrial pellet was resuspended in 0.07 ml of albumin-free washing buffer and stored on ice. The mitochondrial protein content was measured with a Lowry DC kit (Bio-Rad, Hercules, CA) according to manufacturer's instructions. To control for mitochondrial quantity and quality, mitochondria-specific protein markers (Mn Superoxide-dysmutase [MnSOD] and cytochrome oxidaze IV [COX IV]) were quantified by Western blotting in randomly selected samples from naïve mice ($n = 4$) and from mice exposed to hyperoxia for 2 week ($n = 4$). Briefly, 5 μg of

mitochondrial protein was loaded for electrophoresis followed by incubation with primary antibodies, MnSOD (Abcam, Cambridge, MA) and COX IV (Sigma-Aldrich, St. Louis, MO) overnight at 4°C. The immunoexpression of MnSOD and COX IV was identified by a chemiluminiscence detection assay. To assess mitochondrial structural integrity after isolation, mitochondria from naïve 18-day-old mice ($n = 3$) and hyperoxia-exposed mice (Group 2, $n = 2$) were examined under electron microscopy. Briefly, mitochondrial pellets were fixed in 2.5% glutaraldehyde and 4% paraformaldehyde in 0.1 M cacodylate buffer (pH 7.4) at 4°C. After fixation with 1% osmium tetroxide in 0.1 M cacodylate buffer, the pellet was dehydrated and embedded in Epon-Araldite. Ultrathin sections were cut using a Reichert Ultramicrotome (C. Reichert Wien, Vienna, Austria), stained with uranyl acetate, lead citrate and examined under a JEOL 1200 electron microscope (JEOL, Peabody, MA).

Measurement of mitochondrial respiration was performed using a Clark-type electrode (Oxytherm; Hansatech Instruments, Norfolk, UK) at 32°C. Mitochondria (0.065 mg of protein) were loaded into 0.4 ml of respiration buffer: 200 mM sucrose, 25 mM KCl, 2 mM K_2HPO_4, 5 mM HEPES-KOH (pH 7.2), 5 mM $MgCl_2$, 0.2 mg/ml of BSA, 30 μM Ap_5A(P^1,P^5-di(adenosine 5′)-pentaphosphate (an inhibitor of adenylate kinase), 10 mM glutamate, and 5 mM malate. The phosphorylating respiration (State 3) was initiated with 100 nmol of ADP. To dissect direct contribution of electron transport chain to mitochondrial O_2-consumption rate, 35 nmol of 2′4′dinitrophenole (DNP) was added at resting respiration (State 4). Rates of O_2 consumption were expressed in nmol O_2/mg mitochondrial protein/minute. The respiratory control ratio (RCR) was calculated as the ratio of the State 3 to the State 4 respiration rate recorded after phosphorylation of ADP has been completed. The ADP:O ratio was calculated as the amount of added ADP expressed in nmoles divided by the amount of oxygen atoms (nmoles of O_2 multiplied by 2) consumed during ADP-accelerated State 3 respiration. Mitochondrial ATP-production rate was measured in mitochondrial isolates as described (18) with modification. The ATP content was measured using bioluminescence assay (Molecular Probes, Eugene, OR) as described (19). Mitochondrial isolates (0.05 mg of protein) were placed in Clark's-type electrode chamber containing respiration buffer (0.4 ml) and substrates (malate-glutamate). In control (vehicle-treated) mice mitochondrial ATP content was measured prior to supplementation of ADP and at 1 minute after completion of ADP-phosphorylation. In experimental (hyperoxia or pyridaben exposed) littermates, mitochondrial ATP content was measured before supplementation of ADP and during ADP phosphorylation, at the time exactly corresponding to the time point (mean = 7.2 min) at which control mitochondria were sampled for ATP-content. Thus, the same period of time was allotted for each mitochondrial sample to phosphorylate the same amount (100 nmol) of ADP to ATP. Because respiration buffer was supplemented with Ap_5A (an inhibitor of adenylate kinase), the amount of ATP upon completion of phosphorylation is expected to be proportional to the amount of ADP available for phosphorylation. The mean value of ATP yield from 100 nmol of ADP in mitochondria from vehicle-treated mice ($n = 4$) was 118 nmol. The ATP-production rate was estimated as follows: [ATP-content measured after supplementation of ADP] – [ATP-content before supplementation of ADP] / [the mean value of time needed to complete ADP-phosphorylation in control samples]. The ATP-production rate in experimental (pyridaben- or hyperoxia-exposed) littermates was expressed as a percentage of mean values (100%) in vehicle-treated controls.

Complex I Activity Assay

Complex I activity was measured spectrophotometrically as rotenone-sensitive NADH:Q1 reductase (20). The reaction buffer was 2 mM HEPES (pH 7.8), 100 μM NADH, and 100 μM coenzyme Q1. Frozen–thawed mitochondria were homogenized in 2 mM HEPES buffer (pH 7.8) mixed with the reaction buffer in a 96-well plate, and the absorbance changes at 340 nm were followed for 10 minutes with a plate reader SpectraMax M5 (Molecular Devices, Sunnyvale, CA). In control incubations, the reaction buffer was supplemented with 2 μM rotenone. The activity of C-I was calculated as the difference between the rates of NADH oxidation ($E^{340}_{(mM)} = 6.22 \times cm^{-1}$) in the absence and in the presence of rotenone and presented in nmoles NADH/min/mg of mitochondrial protein. A separate cohort of P6 naïve and hyperoxic mice was used for C-I activity measurement. C-I activity was not measured in three mice exposed to hyperoxia for 2 weeks due to insufficient sample volume.

Statistical Analysis

Data are expressed as mean ± SEM. Student's *t* test analysis was used for comparative analysis of alveolarization and mitochondrial function in study groups at each time point. To compare changes in mitochondrial function and pulmonary histopathology over the duration of the experiment, one-way ANOVA with Fisher's *post hoc* analysis was used. Values were considered significantly different if $P < 0.05$.

RESULTS

Morphological Integrity of Mitochondrial Isolate

Electron microscopy of mitochondrial isolates revealed relatively intact fraction of organelles obtained from naïve and hyperoxic mice (Figure 1B). Comparative analysis for markers of mitochondrial quantity in the samples obtained from mice after 2 weeks of hyperoxia and their naïve littermates demonstrated no quantitative differences in organelles (Figure 1C).

Pulmonary Histopathology and Mitochondrial Function during Hyperoxia

Histopathologic analysis in naïve P3 mice revealed markedly underdeveloped lungs at a saccular stage of development (Figure 1D). After 72 hours of exposure, hyperoxic mice exhibited a significant delay in alveolar development; the RACs in these (P6) mice was not significantly different from that in P3 naïve mice (Figures 1D and 1E). In contrast, their age-matched naïve counterparts demonstrated significantly increased RACs compared with P3 naïve mice and hyperoxic P6 mice (Figures 1D and 1E). This alveolar developmental delay was associated with significant inhibition of C-I activity, reduction in O_2 consumption rates during resting (State 4), phosphorylating (State 3), and DNP-accelerated respiration (Figures 2A and 2E). After 72 hours of hyperoxic exposure, the respiratory control ratio was significantly decreased (Figure 2C); however, the ADP:O ratio exhibited only a trend ($P = 0.06$) toward reduction (Figure 2D) compared with their naïve littermates.

After 2 weeks of hyperoxic exposure, mice exhibited significantly decreased RACs compared with naïve littermates (Figures 1D and 1E). Of note, the RACs in these hyperoxic P18 mice did not differ ($P = 0.6$) from that in P6 mice subjected to hyperoxia for 72 hours. In contrast, naïve P18 mice demonstrated age-appropriate alveolar development (Figures 1D and 1E). Pulmonary mitochondria isolated from mice with arrested alveolarization continued to demonstrate significantly reduced mitochondrial O_2 consumption rates during phosphorylation of ADP and during respiration accelerated by DNP compared with naïve littermates (Figures 2A and 2B). The RCR and activity of C-I was also significantly reduced compared with naïve littermates (Figures 2C and 2E). Mice exposed to hyperoxia for 2 weeks (P18) exhibited significantly poorer coupled oxidative phosphorylation as their resting (State 4) respiration rate was significantly ($P = 0.004$) greater compared with that in P6 mice subjected to hyperoxia for 72 hours. In contrast, the State 3 and DNP rates were not significantly different in mice exposed to hyperoxia for 72 hours or for 2 weeks (Figure 2A). The ADP:O ratio after 2 weeks of hyperoxic exposure was significantly ($P = 0.0002$) decreased compared with that after 72 hours of hyperoxia (Figure 2D).

Compared with their naïve counterparts, mice subjected to hyperoxia for 2 weeks and allowed to recover for 3 weeks demonstrated significantly reduced RAC. However, compared with the mice exposed to hyperoxia without recovery, these mice exhibited a significant improvement of their pulmonary alveolarization (Figures 1D and 1E). There were no difference in RACs and mitochondrial function between naïve P18 mice and naïve P39 mice used as a littermate controls for mice exposed to

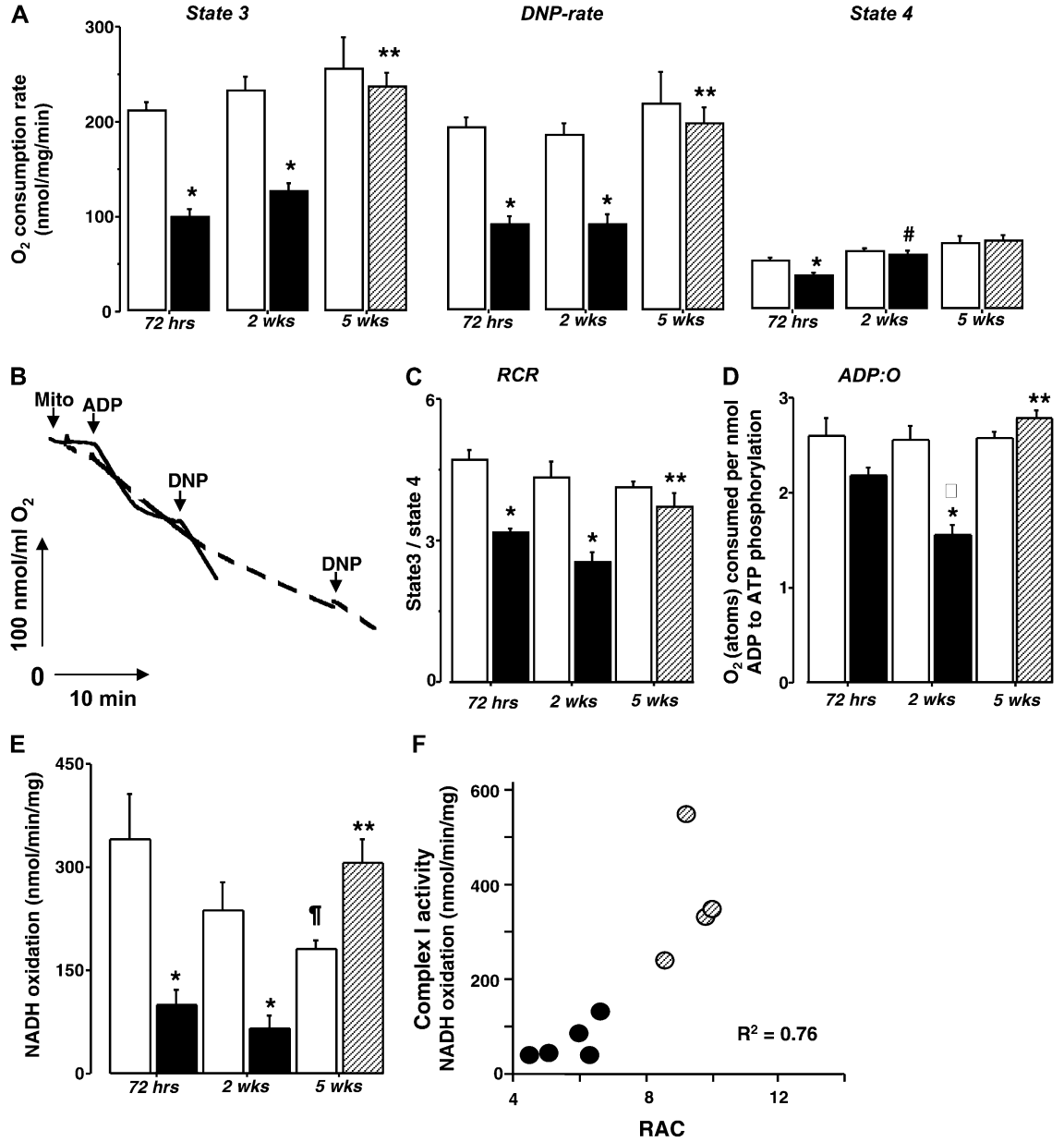

Figure 2. (*A*) Pulmonary mitochondrial respiration rates during phosphorylation of ADP (State 3), after acceleration by DNP (DNP-rate), and during resting (State 4) respiration in naïve (*open bars*) and hyperoxia-exposed mice (*solid bars*) measured: at 72 hours (naïve $n = 4$, hyperoxic mice $n = 5$), at 2 weeks (naïve $n = 6$, hyperoxic mice $n = 7$), and after 3 weeks of recovery (*hatched bars*, naïve = 4, hyperoxic mice $n = 4$). (*B*) Representative recording of mitochondrial respiration in a mouse subjected to hyperoxia for 2 weeks (*dashed line*) and naïve mouse (*solid line*). Time-points at which mitochondria, ADP, and DNP were added are indicated. (*C* and *D*) RCR and ADP:O ratio in mice subjected to hyperoxia for 72 hours, 2 weeks (*solid bars*), and after 3 weeks of recovery (*hatched bar*) compared with naïve littermates (*open bars*). (*E*) Complex I activity in pulmonary mitochondria isolated at 72 hours of hyperoxia (*solid bar*, $n = 5$) compared with naïve mice (*open bar*, $n = 4$), at 2 weeks of hyperoxia (*solid bar*, $n = 5$) compared with naïve mice (*open bar*, $n = 5$), and after 3 weeks of recovery in RA (*hatched bar*, $n = 4$) compared with naïve littermates (*open bar*, $n = 4$). (*F*) Correlation between RAC and C-I activity in mice subjected to hyperoxia for 2 weeks (*solid circles*) and in mice recovered for 3 weeks after 2 weeks of hyperoxia (*hatched circles*). All data are mean ± SEM. $^{*}P < 0.01$ compared with naïve littermates, $^{**}P < 0.01$ compared with mice subjected to hyperoxia for 2 weeks, $^{\P}P = 0.04$ compared with P6 naïve mice, $^{\#}P = 0.004$ compared with mice subjected to hyperoxia for 72 hours, $^{*}P = 0.0002$ compared with mice exposed to hyperoxia for 72 hours.

hyperoxia (Groups 2 and 3, Figures 1D and 1E). In parallel with histologic lung recovery, pulmonary mitochondria in mice allowed to recover after hyperoxia demonstrated significantly improved phosphorylating and DNP-accelerated respiration rates (Figure 2A), RCR, and ADP:O (Figures 2C and 2D) compared with the mice subjected to hyperoxia without recovery. Unexpectedly, naïve mice demonstrated a gradual decrease in their pulmonary C-I activity with advancing postnatal age (Figure 2E). In contrast, hyperoxic mice after 3 weeks of recovery exhibited a dramatic activation of C-I in their lungs compared with that in hyperoxic mice without recovery (Figure 2E). Linear regression analysis in the combined group of mice (hyperoxia for 2 wk + hyperoxia for 2 wk and recovery for 3 wk) revealed very strong correlation ($r^2 = 0.76$) between radial alveolar counts and C-I activity in pulmonary mitochondria (Figure 2F). Because P6 mice demonstrate a natural "developmental" difference in

alveolarization compared with P18 or P39 (mice with a completed alveolarization [12]), P6 mice subjected to hyperoxia were not included in this analysis.

Direct Inhibition of C-I Results in Arrested Alveolarization

As expected, inhibition of C-I by exposure mice to pyridaben resulted in significant inhibition of phosphorylating, ADP-accelerated, and resting respiration rates compared with vehicle-treated littermates (Figure 3A). The extent of this mitochondrial dysfunction to generate ATP in mice exposed to pyridaben for 72 hours was very similar to that observed in mice exposed to hyperoxia for 72 hours (Figures 3A and 3B). Indeed, compared with vehicle-treated controls, lung mitochondria from mice exposed to pyridaben or hyperoxia exhibited significantly decreased ATP production rates, by 35% and 40%, respectively (Figure 3B). An extremely tight ($r^2 = 0.98$) correlation was observed between phosphorylating respiration rate and ATP production rate in mitochondria isolated from pyridaben- or hyperoxia-exposed mice and vehicle-treated littermates (Figure 3C). Most importantly, however, exposure to hyperoxia or pyridaben resulted in the same changes in pulmonary phenotype—a significant delay of alveolar development assessed by RACs and Lms (Figures 4A–4C). The continuation of pyridaben exposure for 2 weeks resulted in remarkable simplification of pulmonary architecture, significantly decreased RACs, and increased Lms compared with vehicle-treated controls (Figures 4A–4C). This extended exposure to pyridaben resulted in a significant inhibition of mitochondrial ATP production rate defined by reduced ADP-phosphorylating respiration compared with vehicle-exposed controls (Figures 3A and 4D). However, when pyridaben exposure for 72 hours was followed by 2 weeks of recovery, pulmonary mitochondria demonstrated a full restoration of ATP-generating capacity defined by normalization of the ADP-phosphorylating respiration rate compared with the age-matched vehicle-treated mice (Figure 3A). This restoration of mitochondrial electron transport chain after 2 weeks of recovery from pyridaben exposure coincided with normal pulmonary development; RACs and Lms in these mice did not differ from that in their vehicle-treated controls (Figures 4A–4C). After a prolonged exposure to pyridaben, no significant difference in ADP:O ratio was detected between pyridaben-exposed mice and their vehicle-treated controls (Figure 4E).

DISCUSSION

This study investigated how immature lungs lose their ability to develop in response to exogenous stress. We used hyperoxia to induce BPD-like changes in immature mice. After 4 weeks of hyperoxia (65% or 85% O_2), mice exhibit histologic and functional changes seen in human neonates with BPD: decreased alveolarization, respiratory acidosis, increased lung resistance, and decreased lung compliance (11, 21). Because alveolarization in mice is completed by 2 to 3 weeks of postnatal age (12), we shortened hyperoxic exposure to 2 weeks. This study demonstrates that hyperoxia-induced alveolar developmental arrest is strongly associated with inhibition of mitochondrial phosphorylating respiration, the most effective pathway in generation of ATP in mammalian cells. *In vivo* control over the rate of

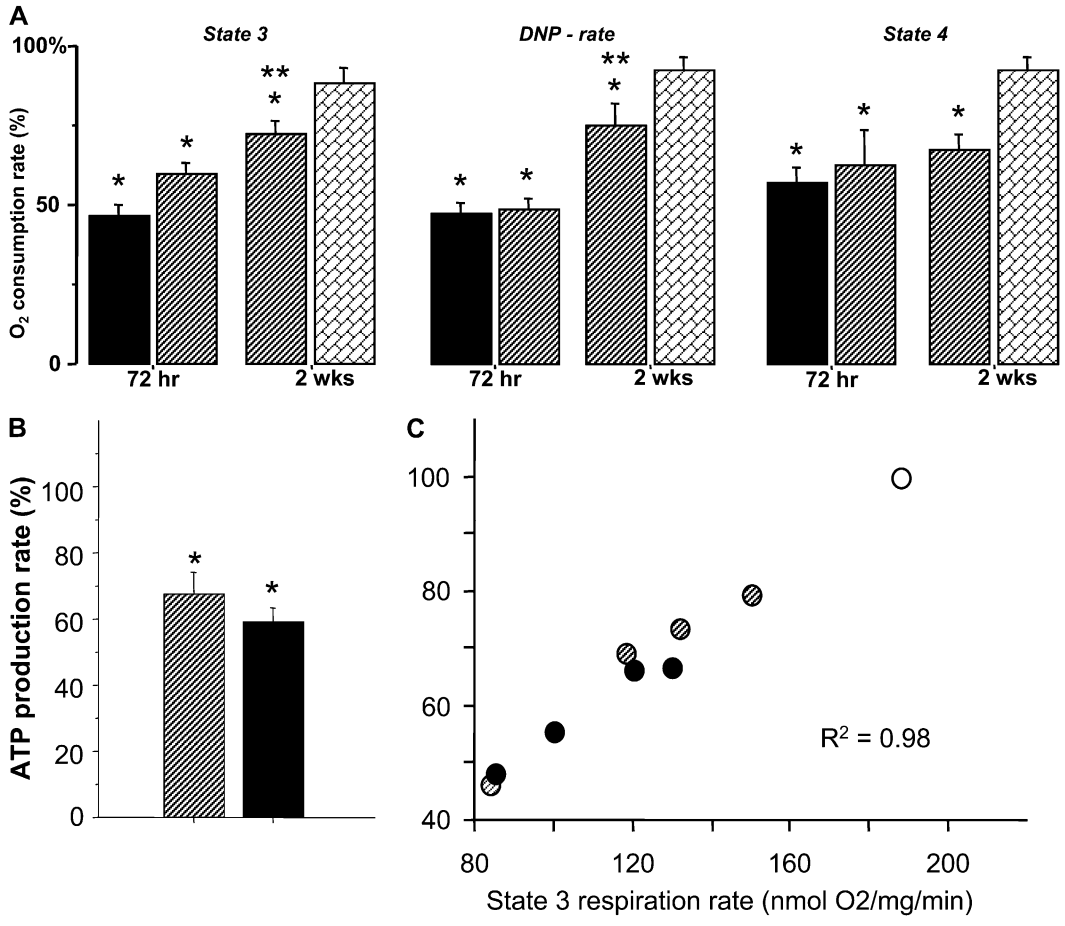

Figure 3. (*A*) Respiration rates in pulmonary mitochondria isolated from mice subjected to hyperoxia (*solid bar*, $n = 8$), pyridaben (*hatched bar*, $n = 6$) for 72 hours or 2 weeks ($n = 5$ in each group) compared with mice recovered from 72 hours of pyridaben exposure for 2 weeks (*bricked bar*, $n = 6$). Data expressed as percentage of mean values (100%) in vehicle-treated littermates ($n = 5$ for each age group). $^*P < 0.05$ compared with vehicle controls, $^{**}P < 0.01$ compared with 72 hours of pyridaben exposure. (*B*) ATP-production rate in mitochondria after 72 hours of exposure to pyridaben (*hatched bar*, $n = 4$) or hyperoxia (*solid bar*, $n = 5$). Data expressed as percentage of mean value (100%) in vehicle-treated littermates. (*C*) Correlation between phosphorylating respiration and ATP production rates: *open circle*, the mean value of State 3 respiration rate in vehicle-treated mice ($n = 4$); *hatched circles*, pyridaben; *solid circles*, hyperoxia-exposed mice. All data are mean ± SEM. $^*P \leq 0.03$ compared with vehicle-treated controls.

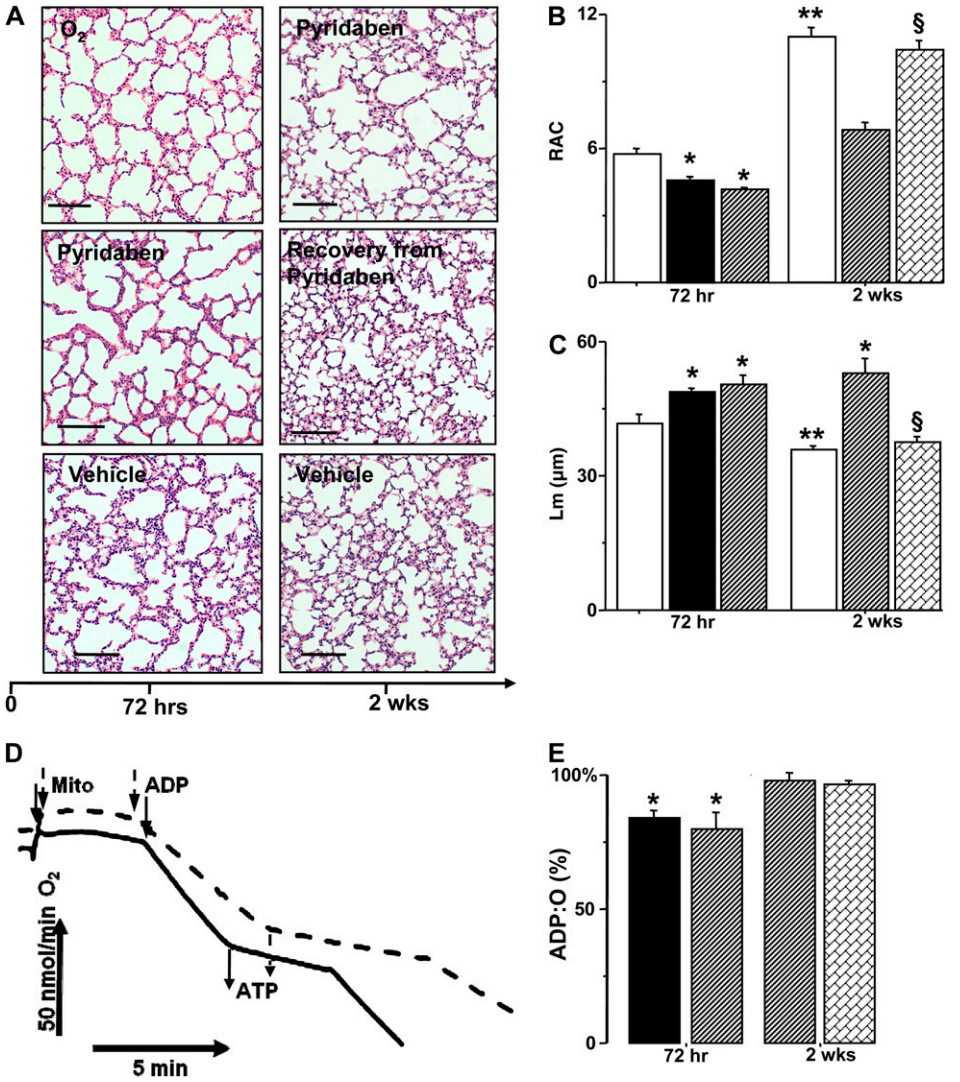

Figure 4. (*A*) Representative images of lung sections in mice exposed to hyperoxia (O_2), pyridaben for 72 hours or 2 weeks, and mice allowed to recover after 72 hours of pyridaben exposure compared with age-matched vehicle-treated controls. *Scale bar* = 500 μm. (*B* and *C*) RAC and Lm in mice subjected to hyperoxia (*solid bar*, $n = 8$), pyridaben (*hatched bar*, $n = 6$) for 72 hours or 2 weeks ($n = 5$), and in mice after recovery from 72 hours of pyridaben exposure (*bricked bar*, $n = 6$) compared with vehicle-treated controls (*open bar*, $n = 4$ and $n = 6$). (*D*) Recording of mitochondrial respiration in mouse subjected to pyridaben for 2 weeks (*dashed line*) and vehicle-treated littermate (*solid line*). Time points at which mitochondria and ADP were added, and end-points of ATP production, are indicated. (*E*) ADP:O ratio (% of mean value in vehicle-treated controls, $n = 6$) in mitochondria from mice exposed to hyperoxia for 72 hours (*solid bar*, $n = 5$), pyridaben (*hatched bar*, at 72 h $n = 6$ and at 2 wk $n = 5$), and mice recovering from 72 hours of pyridaben exposure (*bricked bar*, $n = 6$). All data are mean ± SEM. $^{*}P \leq 0.002$ compared with age-matched vehicle-treated controls, $^{**}P \leq 0.03$ compared with P6 vehicle-treated controls, $^{\S}P < 0.04$ compared with mice exposed to pyridabed for 2 weeks.

phosphorylating respiration is shared between (*1*) the reactions generating electrochemical proton gradient ($\Delta\mu H^+$) (depends on the activity of proton-pumping electron chain complexes), (*2*) the reactions of substrate dehydrogenases (supplying reducing equivalents for the respiratory chain), and (*3*) the reactions consuming the $\Delta\mu H^+$ (such as ATP-ase and ADP/ATP translocator) (22, 23). In the presence of saturating concentrations of NAD-linked substrates and phosphate, the maximum respiration rate in State 3 is not limited by the activity of ATP-phosphorylating system (24) or substrate dehydrogenases (25). This means that in our study a maximum respiration rate in State 3 depended primarily on the activity of electron chain complexes (26). Mitochondria isolated from lungs exposed to hyperoxia compared with naïve littermates exhibited a significantly inhibited respiration during both phosphorylation of ADP and uncoupled respiration induced by DNP. This indicates that hyperoxia inhibits electron transport in the respiratory chain and results in impaired oxidative phosphorylation. This observation is in agreement with our finding that enzymatic activity of Complex I is significantly reduced in lung mitochondria isolated from hyperoxia-exposed mice. Moreover, our study demonstrates a strikingly tight correlation between Complex I activity and severity of alveolar developmental arrest. Indeed, when Complex I in pulmonary mitochondria was inhibited by the exposure to pyridaben, mice also demonstrated significant delay in alveolar development. Because pyridaben specifically inhibits C-I activity and, therefore, electron transport in the respiratory chain, we expected to find depressed mitochondrial respiration and ATP production rates using NAD-linked substrates in mice after pyridaben exposure. The cessation of pyridaben exposure resulted in significant recovery of mitochondrial function associated with normalization of alveolar development. In contrast, mice subjected to pyridaben for an extended period of time (2 wk) exhibited an arrested alveolarization. It is remarkable that the degree of alveolar developmental delay and recovery in the pyridaben-exposed mice was strikingly similar to that in the hyperoxia-exposed counterparts. The exposure to pyridaben in this study was designed to obtain direct evidence that mitochondrial dysfunction result in alveolar developmental arrest. However, an inhibiting effect of pyridaben on C-I is not tissue specific. In this study, mice exposed to pyridaben for 2 weeks demonstrated a significantly ($P = 0.03$) decreased body weight (6.12 ± 0.99 g versus 7.39 ± 0.52 g) and significantly greater mortality rate (chi square $P = 0.04$) compared with their vehicle-treated controls. Similarly, hyperoxia-induced lung injury is associated with poor weight gain and significantly higher mortality rates (11, 21). Thus, the same phenotype—an arrested alveolarization, pulmonary mitochondrial dysfunction, and retarded growth—has been induced by two distinctively different experimental challenges (exposure to hyperoxia or pyridaben). This strongly

suggests a pathogenic role of mitochondrial dysfunction in hyperoxia-induced alveolar developmental arrest.

It is noteworthy that significantly decreased ADP:O ratio was observed only after 72 hours of pyridaben exposure. After an extended (2 wk) exposure to pyridaben, pulmonary mitochondria exhibited an ADP:O ratio similar to that in vehicle-treated counterparts. Hyperoxia, however, was associated with markedly ($P = 0.06$) decreased ADP:O ratio at 72 hours, which significantly ($P = 0.01$) worsened after 2 weeks of exposure. The ADP:O ratio reflects how effectively mitochondrial respiratory chain consumes O_2 to phosphorylate ADP to ATP and decreases if mitochondrial respiration is poorly coupled with phospholylation of ADP. Hyperoxic exposure for 2 weeks resulted in significant uncoupling of mitochondrial respiration, which can explain the altered ADP:O ratio. In our experiments, exposure to pyridaben, initially, resulted in a significantly ($P = 0.03$) poorer respiratory control ratio compared with vehicle-treated controls (data not shown). This may explain the significantly reduced ADP:O ratio in mice exposed to pyridaben for 72 hours. Unexpectedly, after 2 weeks of exposure to pyridaben, those mice that survived this prolonged exposure to C-I inhibitor demonstrated markedly improved respiratory control in their lung mitochondria (data not shown). The continuation of pyridaben exposure for 2 weeks may have resulted in adaptational changes (e.g., up-regulation of C-I proteins), which reduced the sensitivity of the respiratory chain to an inhibiting effect of pyridaben. Indeed, the State 3 respiration rate measured at 2 weeks of exposure was significantly ($P = 0.01$) greater compared with that measured at 72 hours of pyridaben exposure, while State 4 respiration rate did not ($P = 0.56$) differ. Therefore, after 2 weeks of exposure to pyridaben, mitochondrial respiratory control improved compared with that in mice exposed to C-I inhibitor for 72 hours, and did not differ from that in vehicle-treated littermates, which might explain the unaffected ADP:O ratio. Using rat liver mitochondria, other investigators reported that exposure to C-I inhibitors significantly inhibited phosphorylating respiration; however, it had no effect on the ADP:O ratio (27). We believe that the experiments with pyridaben provided the most direct evidence to support our hypothesis because the phosphorylating respiration remained significantly inhibited at 2 weeks of the exposure. This implies that the rate of ATP production was significantly slowed, although the amount of O atoms per phosphorylation of one mole of ADP was not altered. Indeed, the mitochondrial phosphorylating respiration rate (not ADP:O ratio) tightly correlated ($r^2 = 0.98$) with the rate of ATP production.

A pathogenic link between alveolar simplification and reduced ATP production rate is suggested on the basis of data obtained using lung mitochondria isolated from their natural environment. In lungs, Ahmad and coworkers reported that 96 hours of hyperoxic exposure to human epithelial-like cells (A549) in culture resulted in significant depletion of cellular ATP content, as well as decreased mitochondrial membrane potential and respiration rates. All of these were associated with growth arrest and excessive cellular death (9). Of note, hyperoxia has been shown to be detrimental for pulmonary growth not only during lung development, but also during compensatory growth after lobectomy (28).

The mechanism for inhibition of mitochondrial electron transport chain during hyperoxic exposure is uncertain. A study by Li and colleagues (29) demonstrated that respiration-deficient (ρ°) HeLa cells lacking mitochondrial DNA exhibited significantly better growth rate and viability during exposure to 80% O_2 compared with wild-type counterparts. This was accompanied by reduced production of reactive oxygen species (ROS) from electron transport chain and intact aconitase activity in (ρ°) HeLa cells compared with wild-type HeLa cells (29). This work provides evidence that enhanced mitochondrial ROS production may be responsible for the damage (inhibited aconitase activity) of the mitochondrial matrix. Recently, Morton and coworkers demonstrated a profound loss of mitochondrial aconitase activity in lungs obtained from premature baboons with hyperoxia-induced BPD (30). These data suggest that one of the potential mechanisms for mitochondrial dysfunction in our model is intramitochondrial oxidative damage.

Unexpectedly, we found that C-I activity was highest in P6 naïve mice and gradually declined with age, being significantly lower in P39 mice compared with P6 mice. We were not able to find data on C-I activity and pulmonary development. In murine heart, kidney, and muscle, the activity of C-I was reported to be the highest in young animals with a gradual reduction with the age (31–33). In humans, C-I activity in muscle mitochondria was greater in premature neonates compared with older infants and children (34). Of note, in our model a dramatic surge in C-I activity coincided with active alveolar redevelopment during recovery from hyperoxic stress. Considering (*1*) a very tight correlation between C-I activity and RACs in hyperoxia-exposed mice, and (*2*) the ability of pyridaben to delay alveolarization, we propose that the C-I plays a critical role in mitochondrial support for pulmonary development.

In this study we examined a heterogeneous population of mitochondria derived from a variety of cells. We assumed that mitochondria in our isolates mostly represented organelles from epithelial-type cells, as these cells are abundant in the developing lungs. However, it is possible that some mitochondria derived from endothelial cells. Experiments using isolated pulmonary endothelial (35) and epithelial-like cells (9) demonstrated results very similar to ours. The immunoblot analysis of mitochondrial isolates revealed no difference between naïve and hyperoxic mice, suggesting that hyperoxia did not affect mitochondrial integrity. It has been reported that in rats, severe ($F_{I_{O_2}} > 0.95$) hyperoxic exposure for 48 hours did not change the number of mtDNA copies and the ratio between nuclear and mitochondrial DNA (36). This implies a stability of the mitochondrial count in response to hyperoxia. Thus, in our experiments the difference in mitochondria between experimental and control mice is only functional, and not quantitative.

In conclusion, our report is the first to demonstrate that lungs from neonatal mice exposed to hyperoxia exhibit mitochondrial dysfunction in ATP production, which has tight temporal relationship with alveolar developmental arrest and recovery. Moreover, a direct inhibition of mitochondrial oxidative phosphorylation resulted in the same histopathologic changes in lungs—alveolar developmental arrest. Thus, this study provides a line of evidence for the mechanistic role for mitochondrial bioenergetic failure to maintain normal lung development in neonates with BPD.

Conflict of Interest Statement: None of the authors has a financial relationship with a commercial entity that has an interest in the subject of this manuscript.

References

1. Baraldi E, Filippone M. Chronic lung disease after premature birth. *N Engl J Med* 2007;357:1946–1955.
2. Van Marter LJ. Progress in discovery and evaluation of treatments to prevent bronchopulmonary dysplasia. *Biol Neonate* 2006;89:303–312.
3. Brunton JA, Saigal S, Atkinson SA. Growth and body composition in infants with bronchopulmonary dysplasia up to 3 months corrected age: a randomized trial of a high-energy nutrient-enriched formula fed after hospital discharge. *J Pediatr* 1998;133:340–345.
4. Greer FR, McCormick A. Bone growth with low bone mineral content in very low birth weight premature infants. *Pediatr Res* 1986;20:925–928.
5. Furman L, Hack M, Watts C, Borawski-Clark E, Baley J, Amini S, Hook B. Twenty-month outcome in ventilator-dependent, very low birth

weight infants born during the early years of dexamethasone therapy. *J Pediatr* 1995;126:434–440.
6. Giacoia GP, Venkataraman PS, West-Wilson KI, Faulkner MJ. Follow-up of school-age children with bronchopulmonary dysplasia. *J Pediatr* 1997;130:400–408.
7. Simmer K, Rao SC. Early introduction of lipids to parenterally-fed preterm infants. *Cochrane Database Syst Rev* 2005; (2):CD005256.
8. Sosenko IR, Rodriguez-Pierce M, Bancalari E. Effect of early initiation of intravenous lipid administration on the incidence and severity of chronic lung disease in premature infants. *J Pediatr* 1993;123:975–982.
9. Ahmad S, White CW, Chang LY, Schneider BK, Allen CB. Glutamine protects mitochondrial structure and function in oxygen toxicity. *Am J Physiol Lung Cell Mol Physiol* 2001;280:L779–L791.
10. Morava E, Rodenburg R, Hol F, De Meirleir L, Seneca S, Busch R, van den Heuvel L, Smeitink J. Mitochondrial dysfunction in Brooks-Wisniewski-Brown syndrome. *Am J Med Genet A* 2006;140:752–756.
11. Ratner V, Kishkurno SV, Slinko SK, Sosunov SA, Sosunov AA, Polin RA, Ten VS. The contribution of intermittent hypoxemia to late neurological handicap in mice with hyperoxia-induced lung injury. *Neonatology* 2007;92:50–58.
12. Warburton D, Schwarz M, Tefft D, Flores-Delgado G, Anderson KD, Cardoso WV. The molecular basis of lung morphogenesis. *Mech Dev* 2000;92:55–81.
13. Degli Esposti M. Inhibitors of NADH-ubiquinone reductase: an overview. *Biochim Biophys Acta* 1998;1364:222–235.
14. Cooney TP, Thurlbeck WM. The radial alveolar count method of Emery and Mithal: a reappraisal 2–intrauterine and early postnatal lung growth. *Thorax* 1982;37:580–583.
15. Zeltner TB, Burri PH. The postnatal development and growth of the human lung: II. Morphology. *Respir Physiol* 1987;67:269–282.
16. Thurlbeck WM. Measurement of pulmonary emphysema. *Am Rev Respir Dis* 1967;95:752–764.
17. Caspersen CS, Sosunov A, Utkina-Sosunova I, Ratner VI, Starkov AA, Ten VS. An isolation method for assessment of brain mitochondria function in neonatal mice with hypoxic-ischemic brain injury. *Dev Neurosci* 2008;30:319–324.
18. Drew B, Leeuwenburgh C. Method for measuring ATP production in isolated mitochondria: ATP production in brain and liver mitochondria of fischer-344 rats with age and caloric restriction. *Am J Physiol Regul Integr Comp Physiol* 2003;285:R1259–R1267.
19. Slinko S, Caspersen C, Ratner V, Kim JJ, Alexandrov P, Polin R, Ten VS. Systemic hyperthermia induces ischemic brain injury in neonatal mice with ligated carotid artery and jugular vein. *Pediatr Res* 2007;62: 65–70.
20. Starkov AA, Fiskum G. Regulation of brain mitochondrial H2O2 production by membrane potential and NAD(P)H redox state. *J Neurochem* 2003;86:1101–1107.
21. Warner BB, Stuart LA, Papes RA, Wispe JR. Functional and pathological effects of prolonged hyperoxia in neonatal mice. *Am J Physiol* 1998;275:L110–L117.
22. Brown GC, Lakin-Thomas PL, Brand MD. Control of respiration and oxidative phosphorylation in isolated rat liver cells. *Eur J Biochem* 1990;192:355–362.
23. Moreno-Sanchez R, Hogue BA, Hansford RG. Influence of nad-linked dehydrogenase activity on flux through oxidative phosphorylation. *Biochem J* 1990;268:421–428.
24. Kholodenko B, Zilinskiene V, Borutaite V, Ivanoviene L, Toleikis A, Praskevicius A. The role of adenine nucleotide translocators in regulation of oxidative phosphorylation in heart mitochondria. *FEBS Lett* 1987;223:247–250.
25. Moreno-Sanchez R, Devars S, Lopez-Gomez F, Uribe A, Corona N. Distribution of control of oxidative phosphorylation in mitochondria oxidizing nad-linked substrates. *Biochim Biophys Acta* 1991;1060:284–292.
26. Kholodenko BN, Millazhane V, Borutaite VI, Ivanovene LI, Iuodkaite RA, Katiliute ZP, Toleikis AN. *Biokhimiia* 1991;56:1420–1428. (regulation of the heart mitochondrial respiration rate. Comparison of oxidation of succinate and nad-dependent substrates).
27. Gassner B, Wuthrich A, Scholtysik G, Solioz M. The pyrethroids permethrin and cyhalothrin are potent inhibitors of the mitochondrial complex I. *J Pharmacol Exp Ther* 1997;281:855–860.
28. Sekhon HS, Smith C, Thurlbeck WM. Effect of hypoxia and hyperoxia on postpneumonectomy compensatory lung growth. *Exp Lung Res* 1993;19:519–532.
29. Li J, Gao X, Qian M, Eaton JW. Mitochondrial metabolism underlies hyperoxic cell damage. *Free Radic Biol Med* 2004;36:1460–1470.
30. Morton RL, Ikle D, White CW. Loss of lung mitochondrial aconitase activity due to hyperoxia in bronchopulmonary dysplasia in primates. *Am J Physiol* 1998;274:L127–L133.
31. Choksi KB, Nuss JE, Boylston WH, Rabek JP, Papaconstantinou J. Age-related increases in oxidatively damaged proteins of mouse kidney mitochondrial electron transport chain complexes. *Free Radic Biol Med* 2007;43:1423–1438.
32. Choksi KB, Nuss JE, Deford JH, Papaconstantinou J. Age-related alterations in oxidatively damaged proteins of mouse skeletal muscle mitochondrial electron transport chain complexes. *Free Radic Biol Med* 2008;45:826–838.
33. Choksi KB, Papaconstantinou J. Age-related alterations in oxidatively damaged proteins of mouse heart mitochondrial electron transport chain complexes. *Free Radic Biol Med* 2008;44:1795–1805.
34. Honzik T, Wenchich L, Bohm M, Hansikova H, Pejznochova M, Zapadlo M, Plavka R, Zeman J. Activities of respiratory chain complexes and pyruvate dehydrogenase in isolated muscle mitochondria in premature neonates. *Early Hum Dev* 2008;84:269–276.
35. Jones CI, Han Z, Presley T, Varadharaj S, Zweier JL, Ilangovan G, Alevriadou BR. Endothelial cell respiration is affected by the oxygen tension during shear exposure: role of mitochondrial peroxynitrite. *Am J Physiol Cell Physiol* 2008;295:C180–C191.
36. Lightfoot RT, Khov S, Ischiropoulos H. Transient injury to rat lung mitochondrial DNA after exposure to hyperoxia and inhaled nitric oxide. *Am J Physiol Lung Cell Mol Physiol* 2004;286:L23–L29.